Received: 19 September 2023 | Revised: 14 May 2024 | Accepted: 7 June 2024

DOI: 10.1002/jrs.6716

RESEARCH ARTICLE

Journal of RAMAN SPECTROSCOPY WILEY

Surface-enhanced Raman scattering of Cis-(dicyanomethylene) squarate ion on a silver substrate

Flávia C. Marques[1] | **Erix A. Milán-Garcés**[2] | **Vanessa E. de Oliveira**[3] | **Stéfanos L. Georgopoulos**[1] | **Gustavo F. S. Andrade**[1] | **Luiz Fernando C. de Oliveira**[1]

[1]Departamento de Química, Universidade Federal de Juiz de Fora, Núcleo de Espectroscopia e Estrutura Molecular (NEEM), Centro de Estudos de Materiais (CEM), Juiz de Fora, MG, Brazil

[2]Departamento de Física Geral, Instituto de Física, Universidade de São Paulo, São Paulo, SP, Brazil

[3]Departamento de Ciências da Natureza, Universidade Federal Fluminense, Campus de Rio das Ostras, RJ, Brazil

Correspondence
Flávia C. Marques and Luiz Fernando C. de Oliveira, Núcleo de Espectroscopia e Estrutura Molecular (NEEM), Centro de Estudos de Materiais (CEM), Departamento de Química, Universidade Federal de Juiz de Fora, R. José Lourenço Kelmer s/n, Martelos, Juiz de Fora, MG, Brazil, CEP 36036-900.
Email: flavia@ice.ufjf.br; luiz.oliveira@ufjf.br

Abstract

There has been increasing interest in the use of squaraines with different physicochemical properties. However, their applications in nanoplasmonics are limited. For that, detailed information on the interactions of squaraines with plasmonic nanostructures is required. In this work, we have studied the adsorption of the squaraine cis-dicyanomethylene squarate (CDSQ) on the surface of Ag nanoparticles (AgNP). We have combined normal Raman, surface-enhanced Raman scattering (SERS), and DFT calculations to get insights into the configuration of its adsorption. DFT calculations have been carried out using simplified models of different adsorption geometries for comparison with the results of the SERS experiments. A comparison between the relative intensities of the normal Raman and SERS spectra indicates that CDSQ is adsorbed perpendicular to the AgNP surface. The predicted spectra suggest that CDSQ is chemically adsorbed on the silver surface through one of its N atoms.

KEYWORDS

cis-(dicyanomethylene)squarate, DFT, Raman spectroscopy, SERS, silver nanoparticles

1 | INTRODUCTION

Squaraine dyes (Figure 1 a and b) are a promising class of organic compounds with unique electronic and optical properties, making them valuable in various applications such as nonlinear optics, molecular electronics, photodynamic therapy (PDT), and metal–organic framework synthesis.[1–3] Their ability to transport charge and form self-assembled monolayers makes them attractive candidates for use in molecular-scale electronic devices.[4–6] Recent research has highlighted their potential in materials science and organic electronics, and ongoing research has been focused on exploring their use in a wide range of devices.[3,6]

There are several types of squaraine available in the literature, and varying the 'R' group will result in compounds with specific properties. Several squaraine dyes have important issues with solubility and/or stability in aqueous environments; besides, they are subject to significative aggregation processes.[7] The high electron-deficient nature of the oxocarbon core makes the compounds quite susceptible to nucleophilic attack, thus diminishing potential applications in vivo.[7] Conversely, among squaraine dyes, the unique molecular structure of cis-dicyanomethylene squarate ion (CDSQ, Figure 1 (b)), with its π-conjugated system, and electron-withdrawing 'cyano' groups, good solubility, and reasonable stability make it an excellent candidate for developing organic semiconductors and materials with superior charge mobility.[8,9] CDSQ was derived from 1,2-dihydroxy cyclo butene-3,4-dione, also known as squaric acid, as can be seen in Figure 1 (c). One promising avenue for future research on CDSQ is in the field of organic solar cells; the high electron affinity of CDSQ

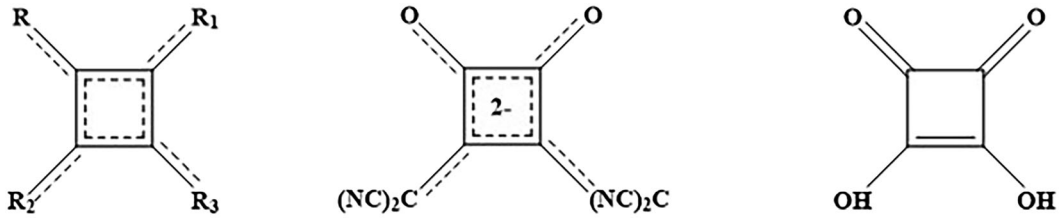

FIGURE 1 Structure of (a) generic squaraines, R: aryl, carbonyl or nitrogen-containing compounds; (b) cis-(dicyanomethylene)squarate ion, and (c) squaric acid.

makes it a suitable acceptor material for use in organic photovoltaic devices, as observed for a series of similar squaraines.[8,10,11] Despite its peculiar properties and relative structural simplicity, compared to other squaraines, there is a lack of robust information concerning CDSQ. There are a few studies specifically addressing this compound.[9,11–13] Such studies have investigated the vibrational properties of CDSQ using normal Raman joint to other techniques, but for the first time, a complete vibrational study involving this compound was carried out, as reported here. It is important to notice that in the last years, our research group has been involved in the structural and vibrational characterization of several different oxocarbon derivatives, including squaraines and other systems, always aiming for the understanding of the interplay between structure and spectroscopic data.[12,14–25]

The study of molecular vibrations is essential for the characterization of organic compounds and materials. Raman spectroscopy is a powerful tool that provides information on the vibrational properties of molecules based on their inelastic scattering of light. However, Raman spectroscopy has some limitations, such as low sensitivity and signal-to-noise ratio, which restrict its applicability in certain situations.[26] One way to overcome these limitations is by using surface-enhanced Raman scattering (SERS).[27] SERS is a technique that uses plasmonic nanostructures of Au, Ag, or Cu to enhance the Raman signal of molecules adsorbed or very close to a plasmonic surface.[28,29] The plasmonic nanostructures generate a high local enhancement of the electrical field of the excitation radiation, which results in a significant enhancement of the Raman signal of the molecules located in their vicinity. The typical enhancement factor for highly active Ag SERS substrates is in the range of 10^6–10^{7}.[30–32] The SERS technique has many advantages over traditional Raman spectroscopy. It can provide information about the structure and orientation of molecules at the surface of the nanostructures[33,34]; in addition, it can detect molecules at much lower concentrations, down to the single-molecule level. [35,36]

SERS studies of squaraines have been reported only in a few cases.[14,37,38] Recently, the interaction of 1,3-dianiline squarate (DSQ) with silver nanoparticles (AgNP) and its adsorption configuration was described using SERS.[14] Here, we performed a detailed Raman spectroscopic analysis and DFT calculations of CDSQ to investigate its vibrational properties and its adsorption on silver nanoparticles; furthermore, the SERS characterization of CDSQ was carried out here for the first time.

2 | EXPERIMENTAL SECTION

2.1 | Chemicals and reagents

Silver nitrate (Sigma-Aldrich, > 99.0%), hydroxylamine hydrochloride (Merck, > 99.0%), sodium hydroxide (Vetec, 97.0%), sodium nitrate (Sigma-Aldrich, > 99.0%), squaric acid (SQ)(Sigma-Aldrich, ≥ 99.0%) were used as received. Aniline (Sigma-Aldrich, 99.0%) was previously bi-distilled. Deionized water ($R = 18.2$ MΩ. cm^{-1}) was used to prepare the aqueous solutions. All other chemical reagents were of analytical grade and obtained from commercial suppliers.

2.2 | Preparation of colloidal AgNP

For synthesizing the AgNP, a procedure described in the literature by Leopold et al. was used.[39] Briefly, 8.5 mg of $AgNO_3$ was dissolved in 45.0 ml of deionized water, and 5.0 ml of hydroxylamine hydrochloride/sodium hydroxide solution (1.5×10^{-2} mol L^{-1}/3.0×10^{-2} mol L^{-1}) was added to the mixture. The mixture is vigorously stirred for 3 minutes at room temperature. The resulting solution turned rapidly to a gray color. The colloidal suspension was stored at 4°C.

2.3 | Preparation of sodium cis-(dicyanomethylene) squarate (Na_2CDSQ)

Step 1: Synthesis of sodium 3,4-dibutoxycyclobut-3-ene-1,2-dione: In a 100 ml round bottom flask with a reflux condenser, a mixture of SQ (1.0 g, 8.77 mmol) and dry n-butanol (30 ml) was heated at reflux for 24 h using a Dean-Stark trap. **Step 2**: After cooling, the next step consists of adding two pre-mixtures to the bottom flask of 'step 1'. *Solution 1*, sodium alkoxide (not isolated): 0.810 g; (8.77 mmol) of metallic sodium and n-butanol (40 ml), to wait for the complete reaction. *Solution 2*: 1.158 g (17.54 mmol) of malononitrile in n-butanol (10 ml), to wait for the complete solubilization. **Step 3:** Both solutions 1 and 2 were added simultaneously to the first flask solution (Step 1); a light yellow powder is obtained. Yield 1.455 g (79.7%). Steps 2 and 3 were performed at 25°C. Elemental analysis of $Na_2C_{10}H_6N_4O_2.3H_2O$ (344.19 g.mol^{-1}) gave the following data: calc. C 34.90, H 2.93, and N 16.28%; found C 35.39, H 2.91, and N 16.37%. Molar absorptivities: 381 nm ($\varepsilon = 4.2 \times 10^4$ mol^{-1}.L.cm^{-1}), shoulder at 346 nm ($\varepsilon = 3.1 \times 10^4$ mol^{-1} L cm^{-1}); 263 nm ($\varepsilon = 2.0 \times 10^4$ mol^{-1} L cm^{-1}); 228 nm ($\varepsilon = 2.6 \times 10^4$ mol^{-1} L cm^{-1}). In the 13C NMR spectrum of Na_2CDSQ, the signals (ppm) at δ 39.21; δ 123.96; δ 173.04, and δ 187.01, were assigned to C-7/8, C-9/10/11/12, C-2/3, and C-1/4, respectively (the numbering of carbon atoms refer to Figure 3 (a)).

2.4 | Characterization

UV–Vis absorption spectroscopy analyses were performed using a Shimadzu UV-1800 spectrometer operating in the region of 200 to 1100 nm using quartz cuvettes with a 5 mm optical path. The UV–Vis of the Na_2CDSQ aqueous solution was obtained in the concentration 2.0×10^{-5} mol L^{-1}.

2.5 | Spectroscopic measurements by SERS and Raman

The Raman and SERS spectra were acquired in a Bruker spectrometer, model SENTERRA. The exciting radiation used was 785 nm, with laser power at a laser head of 100 mW. The laser was focused on the sample by a 50 × magnification objective (NA 0.55), and the integration time was 20 s. For the acquisition of the Raman spectrum of solid Na_2CDSQ, the sample was placed on a rigorously cleaned glass slide. For the Raman spectrum of Na_2CDSQ in an aqueous solution, a 0.16 mol L^{-1} solution was prepared. The SERS spectra were obtained from the preparation procedure for Na_2CDSQ samples, as follows: [50 µl 4.0 mmol L^{-1} Na_2CDSQ + 50 µl 200.0 mmol L^{-1} $NaNO_3$ + 100 µl Ag colloid]. In the literature,[39] the utilization of a 785 nm excitation for SERS acquisition is common practice, particularly with AgNP synthesized using hydroxylamine.

2.6 | Computational details

The calculations were carried out using the Gaussian 09 software package.[40] The geometries of the compounds were optimized in the gas phase at the Density Functional Theory (DFT) level with the B3LYP exchange-correlation functional. The basis sets used for C, O, and N atoms were 6–31 + G(2df), which included the polarization function and diffuse functions to all atoms, except for Ag. For Ag, we employed the LanL2TZ(f)[41] effective core potential, along with its associated basis set. This basis set is characterized by triple zeta valence orbital quality and includes f polarization functions. The frequency and Raman activities calculation was performed at the same level as the optimization step. The computed harmonic frequencies were not scaled, and Raman signals were convolved with Lorentzian functions with a Full Width at Half Maximum (FWHM) of 4 cm^{-1}.

Calculated Raman activities (A_i) were converted to relative Raman intensities (I_i) using the following relationship[35,42]:

$$I_i = \frac{\alpha A_i (\nu_0 - \nu_i)^4}{\nu_i \left(1 - e^{-hc\nu_i/k_b T}\right)} \quad (1)$$

Where ν_0 is the excitation wavenumber (cm^{-1}); ν_i is the vibrational wavenumber (cm^{-1}); T is the absolute temperature; h is the Planck constant; c is the speed of light; k_b is the Boltzmann constant, and α is a factor for adjusting all band intensities and is equivalent to 10^{-12}. The assignment of vibrational modes was carried out using the VEDA 4 (Vibrational energy distribution analysis) program.[43]

3 | RESULTS AND DISCUSSION

3.1 | Vibrational assignment of the Raman spectrum of sodium cis-(dicyanomethylene) squarate

The first Raman spectrum of Na_2CDSQ was reported by de Oliveira et al. using FT-Raman and 1064 nm excitation wavelength.[12] Figure 2 shows a comparison of the

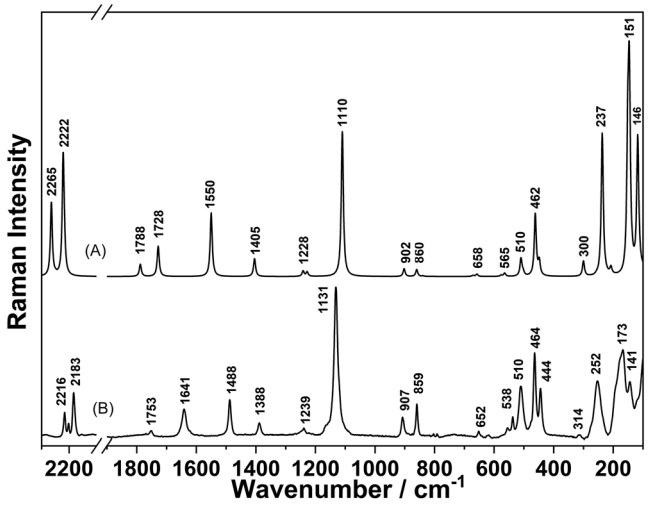

FIGURE 2 (a) Calculated Raman spectrum of CDSQ, and (b) Normal Raman spectrum of solid Na_2CDSQ using 785 nm excitation wavelength.

normal Raman spectrum of Na_2CDSQ in the solid state obtained with a 785 nm excitation line and the predicted Raman spectrum using DFT calculations. Table 1 includes the position of the more intense experimental Raman and infrared bands of solid CDSQ, the calculated wavenumber, Raman activities, and infrared intensities, as well as the corresponding vibrational assignment. The vibrational assignment was carried out based on DFT calculations and on previous vibrational studies of Na_2CDSQ.[12,13] More detailed information can be found in the Supplementary Material (Table S1). The optimized structure of the CDSQ ion in a vacuum is shown in Figure 3a, and its atomic coordinates and detailed structural parameters can be found in Tables S2 and S3, respectively. The electrostatic potential map calculated for the optimized structure, presented in Figure S2 of the Supporting Information file, indicates that the negative charge in the CDSQ anion is distributed throughout the molecule, as commonly observed in conjugated systems. This charge delocalization is facilitated by the presence of alternating single and double bonds, enabling the redistribution of electron density.

The normal Raman spectrum of solid Na_2CDSQ in Figure 2b matches quite well those reported in previous works in terms of the number of active Raman bands, wavenumbers, and relative intensities.[12,13] Raman bands of Na_2CDSQ below 400 cm^{-1} are reported here for the first time. There is an excellent agreement between the calculated and experimental Raman spectra. The recorded Raman spectrum is characterized by a very strong band at 1131 cm^{-1} assigned to ring ν (CC). Strong bands are also observed in the lower frequency region at 173, 252, and 464 cm^{-1} assigned to δ (NCC), δ (CCC), and ν (CC) + δ (NCC) vibrations, respectively. These bands are predicted between the stronger ones in the theoretical spectrum. Other medium and weak intense bands can be observed, for example, at 538, 652, 859, 907, 1239, 1388, 1488, 1641, 1753, 2183, and 2216 cm^{-1}. Very weak bands are also present, as shown in Table 1.

The bands observed at 2183, 2202, and 2216 cm^{-1} correspond to ν (CN) vibrations; the bands at 1641 and 1753 cm^{-1} are assigned to the ν (CO) and ν (CC) + ν (CO) respectively. The carbonyl band at 1753 cm^{-1} is very weak in the normal Raman spectrum of the solid, in agreement with the calculated spectrum and with the reported normal Raman spectra of squarate in solution.[25] The bands at 1239, 1388, and 1488 cm^{-1} have also a contribution from ν (CC), ν (CC), ν (CC) + ν (CO) modes, respectively. The bands at 859 and 907 cm^{-1} are assigned to in-plane δ (CCC) and ν (CC) + δ (CCC). Furthermore, at frequencies below 700 cm^{-1}, the vibrational modes presented a large contribution from ring deformations and torsions. The very weak bands at 620 and 652 cm^{-1} are due to δ (NCC) + δ (CCC) and δ(CCC) vibrations, respectively. The weak bands observed at 510, 538, and 555 cm^{-1} have contributions mainly from τ (NCCC), τ(NCCC) + γ (CCCC), and γ (OCCC) + τ (NCCC), respectively. Another medium-intense band is present at 444 cm^{-1}, corresponding to δ (NCC) + δ (CCC) movements. Except for a few weak bands, the overall normal Raman spectrum of solid Na_2CDSQ is dominated by in-plane vibrational modes.

3.2 | UV–vis spectrum of CDSQ ion on AgNP

The UV–Vis spectra of Na_2CDSQ, AgNP colloid, and Na_2CDSQ:AgNP 1:1 v:v mixture are presented in Figure 4a. The Na_2CDSQ presents a strong absorption band at 381 nm in an aqueous solution, with a shoulder at 346 nm. It is well known from the literature that the electronic bands of CDSQ anion in aqueous solution are related to the $\pi - \pi^*$ electronic transitions in the squarate ring and the CN groups.[12] On the other hand, the localized surface plasmon resonance (LSPR) band of AgNP suspension is observed at 423 nm with a broadband characteristic of the heterogeneous size distribution of nanoparticles, as expected from the AgNP coming from the synthesis protocol by Leopold et al.,[39] used in the present study.

It can be observed in the UV–vis spectrum of Figure 4a, that there is a redshift (from 423 nm to 426 nm) of the absorption maximum of the band attributed to the LSPR of the AgNP upon mixing with the solution of Na_2CDSQ. This shift can be attributed to the adsorption of CDSQ anion on the surface of AgNP

TABLE 1 Wavenumbers (in cm^{-1}) and assignment of main Raman and IR bands of CDSQ ion, calculated at the B3LYP/6-31 + G(2df) level, and the experimental data for Na_2CDSQ (solid).

Exp. wavenumber (cm^{-1}) Solid Raman	Exp. wavenumber (cm^{-1}) Solid IR	Cal. Wavenumber (cm^{-1}) DFT/B3LYP	Raman activity ($Å^4$/amu)	IR (10^{-40} esu^2 cm^2)	Assignment[a]
173 s	-	151	10.86	5.38	δ ($N_{13}C_9C_7$) (14%) + δ ($N_{16}C_{12}C_8$) (14%) + δ ($C_{10}C_7C_9$) (23%) + δ ($C_{12}C_8C_{11}$) (24%)
252 s	-	237	27.52	1.81	δ ($C_{11}C_8C_3$) (14%) + δ ($C_9C_7C_2$) (12%)
444 s	-	448	7.49	0.22	δ ($N_{13}C_9C_7$) (13%) + δ ($N_{16}C_{12}C_8$) (13%) + δ ($C_4C_3C_2$) (15%) + δ ($C_3C_2C_1$) (13%)
464 s	457 w	462	34.10	0.58	ν (C_7C_2) (12%) + ν (C_8C_3) (12%) + ν (C_3C_2) (14%) + δ (NCC) (28%)
510 s	-	510	11.25	6.46	τ ($N_{13}C_9C_7C_2$) (27%) + τ ($N_{14}C_{10}C_7C_2$) (19%) + τ ($N_{15}C_{11}C_8C_3$) (18%) + τ ($N_{16}C_{12}C_8C_3$) (27%)
859 m	863 m	860	9.99	46.71	δ ($C_4C_3C_2$) (14%) + δ ($C_3C_2C_1$) (10%)
907 m	-	902	12.15	0.026	ν (C_2C_1) (11%) + δ ($C_4C_3C_2$) (13%) + δ ($C_3C_2C_1$) (16%)
1131 s	-	1110	306.01	62.31	ν (C_3C_2) (29%) + ν (C_2C_1) (19%) + ν (C_4C_3) (26%)
1388 w	1420 vs	1404	58.30	1310.07	ν (C_7C_2) (32%) + ν (C_8C_3) (32%)
1488 m	1522 s	1550	248.46	1142.60	ν (C_1O_5) (10%) + ν (C_4O_6) (10%) + ν (C_7C_2) (20%) + ν (C_8C_3) (20%) + ν (C_3C_2) (23%)
1641 m	1617/1655 w	1728	146.30	507.45	ν (C_1O_5) (42%) + ν (C_4O_6) (42%)
1753 vvw	1754 m	1788	62.87	622.10	ν (C_1O_5) (33%) + ν (C_4O_6) (33%) + ν (C_3C_2) (11%)
2183 m	2182 m	2222	960.52	307.09	ν (C_9N_{13}) (28%) + ν ($C_{10}N_{14}$) (17%) + ν ($C_{11}N_{15}$) (16%) + ν ($C_{12}N_{16}$) (27%)
2216 m	-	2264	643.57	227.91	ν ($C_{12}N_{16}$) (17%) + ν ($C_{10}N_{14}$) (27%) + ν ($C_{11}N_{15}$) (27%) + ν (C_9N_{13}) (17%)

[a]Assignment based on the potential energy distribution calculated using the software VEDA 4.[43]

ν, stretching; δ, in-plane deformation; τ, torsional; γ, out-of-plane deformation;v, very; s, strong; m, medium; w, weak.

resulting in a significant change in the local refractive index. However, no new band or significative increase in the absorption for longer wavelengths was observed, which indicates that the aggregation state of the AgNP was not strongly affected by interaction with CDSQ. Furthermore, it is also verified a redshift in the electronic transition of CDSQ. This change may be an indication of a charge transfer (CT) between the adsorbed molecule and Ag atom clusters at the nanoparticle surface. To verify whether the CT occurs, we calculated the electronic transitions of the CDSQ and Ag-CDSQ structure using the TD-DFT protocol at CAMB3LYP/6-31G + (2df) level. This combination of functional/basis functions is expected to provide a more accurate asymptotic behavior for CT transitions. Specifically, the CAMB3LYP function is based on the long-range correction of the exchange potential introduced by Tawada et al.[44] and applied to modify the B3LYP functional[45] using the Coulomb-attenuating method (CAM). Figure 4b shows the theoretical absorption spectra obtained for the CDSQ (Figure 3a) compared with the adsorption of CDSQ bound to Ag by one N atom (Figure 3b). The same red-shifting trend was observed, although there is a discrepancy in the transition energies. This result can be attributed to the formation of a CT complex formed between CDSQ and Ag.

The molecular orbital theory was used to verify the possibility of CT between Ag and CDSQ molecules. The highest occupied molecular orbital (HOMO) and lowest unoccupied molecular orbital (LUMO) of Ag-CDSQ (adsorption assumed as the model in Figure 3b) are presented in Figure 4c. It is evident from the molecular orbitals that HOMO is situated at the CDSQ structure and

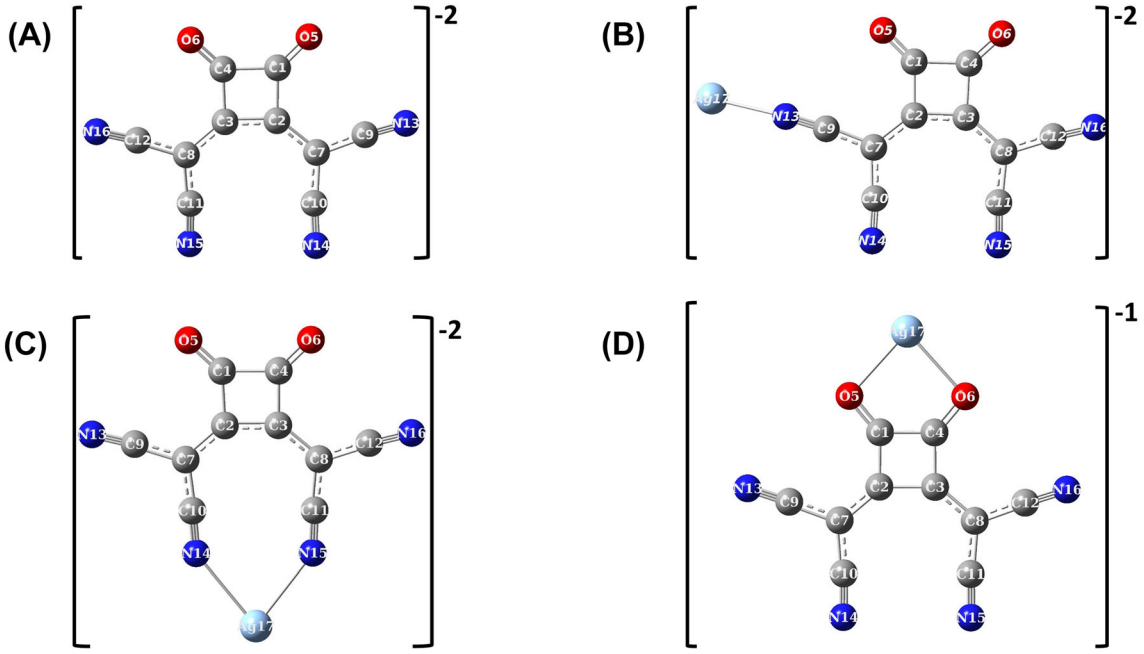

FIGURE 3 Optimized structures of (a) CDSQ ion, and different models for adsorption: (b) Ag − N, (c) N − Ag − N, and (d) O − Ag^{+} − O. Each structure presents the atomic numbering adopted in the assignment of the vibrational spectra.

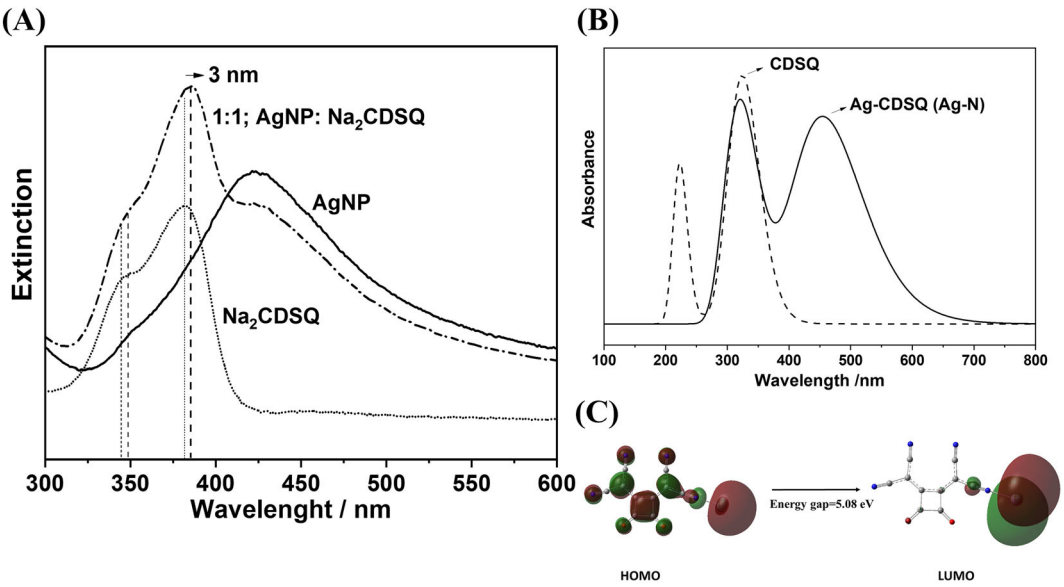

FIGURE 4 (a) Electronic absorption spectra of Na_2CDSQ aqueous solution in the concentration 2.0×10^{-5} mol L^{-1}, AgNP suspension, and solution 1:1; AgNP: Na_2CDSQ, resulting in a final Na_2CDSQ concentration of 2.0×10^{-5} mol L^{-1}; (b) theoretical electronic spectra obtained by TD-DFT calculations at CAMB3LYP/6-31G + (2df) level and (c) molecular orbitals HOMO and LUMO of Ag-CDSQ (assuming adsorption as in the model of Figure 3(b).

extended to the surface of the Ag atom. The LUMO is located effectively in the nitrogen atoms of CDSQ and extended well over the Ag, favoring surface metal-molecule interaction. This is due to the interfacial CT and, therefore, it is reflected in $\pi - \pi^*$ electronic transitions of the squarate ring and the CN groups in the visible region.

3.3 | Normal Raman and SERS spectra of CDSQ ion

The normal Raman spectrum of Na_2CDSQ in solution 0.16 mol L^{-1} and its SERS spectrum using silver nanoparticles (CDSQ at 1.0 mmol L^{-1}) are presented in

Figure 5. The vibrational assignment on the main bands of the normal Raman spectrum of Na_2CDSQ in solution and its SERS spectrum is also found in Table 2. More details are shown in Table S4. In a comparison of the Raman spectrum of Na_2CDSQ in an aqueous solution (Figure 5b) with the Raman spectrum of the solid (Figure 2b), there are several appreciable differences. The major changes occur in the region from 1000 to 1700 cm^{-1}, where some Raman bands are very weak or even absent in the spectrum of the solution. There is also an increase in the linewidth of several bands in comparison with the solid. The broadening differences may have occurred because the molecules in the liquid present more freedom to populate different structural configurations because of their flexibility and interaction with the solvent through different atomic groups. These effects may produce wavenumber shifts for different configurations, resulting in the broadening of the bands when compared to the spectrum of the solid structure where the molecules are in fixed positions with a similar local environment. Similarly for the solid, the more intense Raman bands in the spectrum of the solution occur at 468, 510, and 1132 cm^{-1}. The carbonyl band at 1751 cm^{-1} is also very weak for the molecule in the solution. Another band with contribution from carbonyl vibration absent in solution is the band at 1641 cm^{-1}.

The SERS spectrum of Na_2CDSQ in Figure 5a has several very intense bands as well as variations of band position in comparison with the normal Raman spectrum in solution which suggests not only electrostatic attractions but also chemisorption of CDSQ to the Ag surface. The two strongest bands occur at 260 and 520 cm^{-1}. Other intense bands at 1131, 1550, 1761, and 2222 cm^{-1} are also observed. Interestingly, the bands at 1761 and 2222 cm^{-1} related to stretching vibrations of the carbonyls and cyano groups, respectively, show a drastic increase in their relative intensities. The bands around 2200 cm^{-1} are weak in the spectra of solid and in solution. Similarly, the band around 1750 cm^{-1} is very weak in both normal Raman spectra. Strikingly, the SERS spectrum shows enhancement only of the Raman bands corresponding to in-plane vibrational movements. This result indicates that CDSQ is placed perpendicular to the metallic nanoparticle surface. The observed decrease in the linewidth of the SERS spectrum in comparison with the normal Raman in solution may suggest that the molecule interacts strongly with the surface losing the possibility of being in different structural conformations.

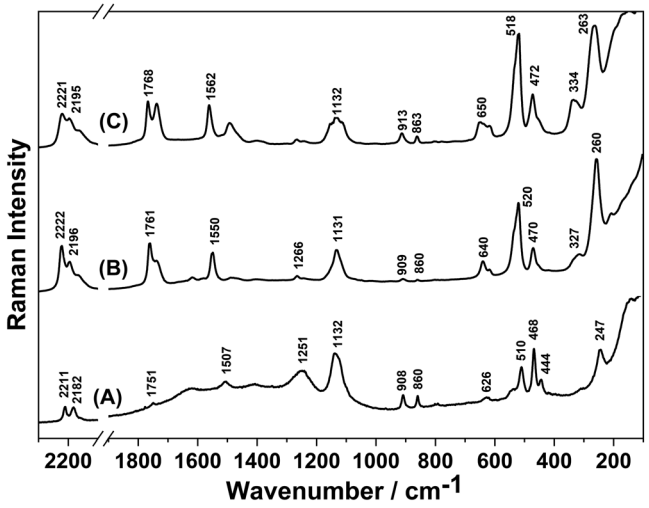

FIGURE 5 (a) Normal Raman spectrum of Na_2CDSQ in an aqueous solution at a concentration of 0.16 mol L^{-1}, (b) SERS spectrum of Na_2CDSQ at a concentration of 1.0 mmol L^{-1} adsorbed on AgNP, and (c) Normal Raman spectrum of CDSQ-Ag^+ in an aqueous solution ((1:1) (Na_2CDSQ: $AgNO_3$)) at a concentration of 0.16 mol L^{-1}.

To account for the direct interaction of the molecule with silver atoms on the surface, a complex of CDSQ with Ag^+ was prepared. The complex was obtained by combining CDSQ and $AgNO_3$ in a 1:1 M ratio, with a solution concentration of 0.16 mol L^{-1}. The normal Raman spectrum of the complex is shown in Figure 5c. The normal Raman spectrum of the complex is very different from that of CDSQ in solution but surprisingly similar to the SERS spectrum, particularly in the number of observed bands as well as in their relative intensity. For example, the positions of the bands assigned to νCN are similar in both spectra. Thus, the differences between the normal Raman and SERS spectra of CDSQ seem to occur due to the changes in the polarizability upon CDSQ interacting with the silver atoms in the nanoparticle surface.

To obtain more insights into the nature of CDSQ adsorption on AgNP, we have carried out DFT calculations representing three possibilities of adsorption through different atomic groups, as illustrated in Figure 3b, c, and d. The metal active sites were modeled simply as Ag adatoms or adclusters, consisting of one or a few Ag atoms, respectively, as stated by Otto et al.[46] and Aroca et al.[47] DFT calculations have often been capable of satisfactorily reproducing the corresponding SERS spectra [48–51]. Initially, we conducted simulations with Ag^0 to mimic a system analogous to metallic silver. While the first two structures exhibited convergence, it is noteworthy that the complex formed by the adsorption of oxygen O-Ag-O did not converge. Notably, the adatoms present on the surface of colloidal silver nanoparticles can be effectively regarded as positively charged. It is important to underline that the adatoms present on the surface of the silver colloidal nanoparticles can be effectively considered positively charged. Therefore, positively

charged sites can be anticipated on the surface of Ag, leading us to utilize the model complex O-Ag^{+}-O. Both approaches could be effectively employed to simulate the real system. The optimized structures, considering CDSQ adsorbed to the Ag atom by the following combinations: Ag−N, N − Ag−N, and O − Ag^{+} − O, are depicted in Figure 3b, c, and d, respectively. Tables S5-S10 (Supporting Information) include the atomic coordinates of the optimized structure and the structural parameters of each model. Tables 2, S15, and S16 (Supporting Information) contain the results of the vibrational frequency calculations.

Figure 6 shows a comparison between the experimental SERS of CDSQ and the predicted theoretical SERS spectra of the three models of adsorption. The results showed that the calculated spectra of the two configurations with the adsorption through the N atoms present frequencies and relative intensities that reasonably agree with those observed in the SERS spectra. The best results were obtained for the Ag−N model (Figure 3b), where only one N atom interacts with the Ag atom. The calculated spectrum of the O − Ag^{+} − O structure (Figure 3d), which considered adsorption through the carbonyl group, has more discrepancies concerning the experimental

TABLE 2 Raman wavenumber/cm^{-1} and assignments of Na_2CDSQ solution, CDSQ-Ag^{+} complex, SERS experimental of CDSQ adsorbed on Ag in 785 nm, and the adsorption model on Ag-N calculated at the B3LYP/6–31 + G(2df) level.

Exp. wavenumber (cm^{-1}) Solution Raman	Exp. wavenumber (cm^{-1}) CDSQ-Ag^{+} complex Raman	Exp. wavenumber (cm^{-1}) SERS	Cal. Wavenumber (cm^{-1}) DFT/B3LYP	Raman activity (Å^4/amu)	Assignment [a]
247 m	263 s	260 s	246	19.42	ν ($Ag_{17}N_{13}$) (10%) + δ ($O_6C_4C_3$) (14%) + δ ($C_8C_3C_4$) (11%) + δ ($C_{11}C_8C_3$) (11%)
468 s	470 m	470 m	466	50.28	ν(C_7C_2) (12%) + ν (C_8C_3) (13%) + ν (C_3C_2) (15%) + δ ($N_{16}C_{12}C_8$) (15%)
510 m	518 s	520 s	512	8.29	δ ($N_{13}C_9C_7$) (20%) + δ ($N_{14}C_{10}C_7$) (20%) + δ ($C_9C_7C_2$) (18%)
626 vw	616 w	617 vw	653	0.83	ν($C_{11}C_8$) (13%) + ν ($C_{12}C_8$) (12%) + δ ($N_{15}C_{11}C_8$) (17%) + δ ($N_{16}C_{12}C_8$) (18%) + δ ($C_{12}C_8C_{11}$) (31%)
-	650 w	640 w	662	8.13	ν (C_9C_7) (11%) + ν ($C_{10}C_7$) (14%) + δ ($N_{13}C_9C_7$) (17%) + δ ($N_{14}C_{10}C_7$) (16%) + δ ($C_{10}C_7C_9$) (31%)
860 w	863 w	860 vw	864	12.65	ν ($C_{12}C_8$) (10%) + δ ($C_4C_3C_2$) (12%)
908 w	913 w	909 vw	900	62.59	ν (C_2C_1) (12%) + δ ($C_4C_3C_2$) (11%) + δ ($C_3C_2C_1$) (16%)
1132 s	1132 s	1131 s	1102/1120	177.40	ν ($C_{11}C_8$) (11%) + ν (C_4C_3) (40%) + δ ($C_4C_3C_2$) (14%) /ν ($C_{10}C_7$) (12%) + ν (C_2C_1) (35%) + δ ($C_3C_2C_1$) (19%) + δ ($O_5C_1C_4$) (10%)
1251 s	1268 vw	1266 vw	1248	90.55	ν (C_9C_7) (21%) + ν ($C_{10}C_7$) (26%) + δ ($C_9C_7C_2$) (12%)
1507 vvw	1562 s	1550 s	1557	580.54	ν (O_5C_1) (11%) + ν (C_7C_2) (17%) + ν (C_8C_3) (24%) + ν (C_3C_2) (26%)
1638 w	1738 s	1738 m	1741	235.68	ν (O_5C_1) (46%) + ν (O_6C_4) (38%)
1751 vvw	1768 s	1761 s	1794	1844.17	ν (O_5C_1) (28%) + ν (O_6C_4) (39%) + ν (C_3C_2) (11%)
2154 sh vvw	2158 m	2163 m	2212.81	2240.65	ν (C_9N_{13}) (66%) + ν ($C_{10}N_{14}$) (21%)
2182 w	2195 m	2196 m	2228	801.79	ν ($C_{11}N_{15}$) (39%) + ν ($C_{12}N_{16}$) (48%)
2211 w	2221 s	2222 s	2271	363.79	ν ($C_{12}N_{15}$) (12%) + ν ($C_{10}N_{14}$) (36%) + ν ($C_{11}N_{15}$) (25%) + ν (C_9N_{13}) (12%)

[a]Assignment based on the potential energy distribution calculated using the software VEDA 4. [43]

ν, stretching; δ, in-plane deformation; τ, torsional; γ, out-of-plane deformation;v, very; s, strong; m, medium; w, weak.

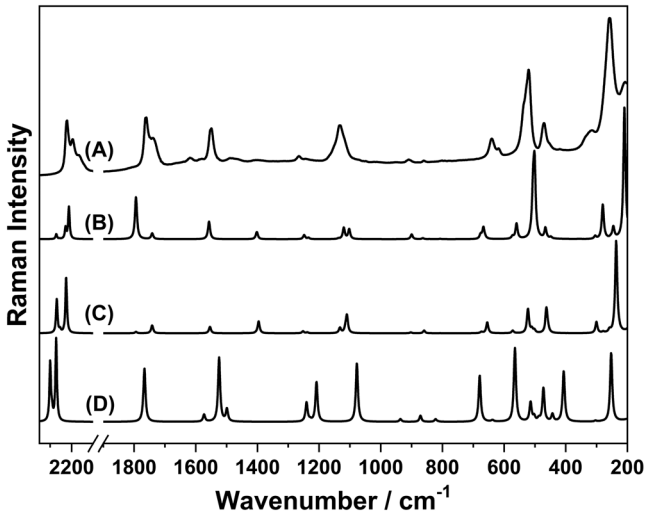

FIGURE 6 (a) Experimental SERS; theoretical spectra of CDSQ on Ag surface using the model (b) Ag−N, (c) N − Ag−N, and (d) O − Ag^{+} − O.

TABLE 3 Mulliken charges of CDSQ anion.

Atom in CDSQ structure*	Charge
C1	−0.107
C2	0.276
C3	0.276
C4	−0.107
O5	−0.398
O6	−0.398
C7	−0.100
C8	−0.100
C9	0.0173
C10	0.0876
C11	0.0876
C12	0.0175
N13	−0.410
N14	−0.365
N15	−0.365
N16	−0.410

*The atom number refers to Figure 2a.

SERS. The nitrogen atom N is more negatively charged than O, based on the evaluation of the Mulliken atomic charges shown in Table 3 (−0.410 for N_{13} and N_{16} and −0.398 for O_5 and O_6). Consequently, it would be expected the N atom to be more favorably bound to the metal. This analysis suggests that the molecule may be adsorbed on the silver surface through the N atom in Ag-N_{13} or Ag-N_{16} configuration. The monodentate bond between the cyano group and metal ions was previously reported by Fabre et al.[9] in the complexation of the dianion 2,4-bis (dicyanomethylene)-cyclobutane-1,3-dione with copper (II) ions. In that study, the authors reported that one copper ion coordinated with each C $(CN)_2$ dicyanomethylene group, forming a Cu-N bond. Oliveira et al.[12] also showed similar results using bis (dicyanomethylene)square interacting with several alkali metals. These data reinforce that the CDSQ molecule can be adsorbed on the silver surface through a monodentate configuration. We also analyzed the formation of the CDSQ complex where two cyano groups are linked to one Ag atom. However, the proposed structure did not reach convergence, probably due to steric hindrance.

Discrepancies in relative intensities are observed, primarily for the modes attributed to νCN, at 2222, 2196, and 2163 cm^{-1}, between experimental and theoretical spectra (Figure 6). The strongest νCN band appears at 2222 cm^{-1}, corresponding to the calculated mode at 2271 cm^{-1}. For all νCN contributions, a more significant contribution from C_9N_{13}, to which the Ag atom is bonded, was expected. However, this mode exhibits a potential energy distribution (PED) of only 12% (see Table 2). The predominant contribution from C_9N_{13} lies in a low-intensity band at 2163 cm^{-1}, attributed to the predicted mode with the highest intensity for nitrile stretching at 2213 cm^{-1}, which presents a PED of 66%. Additionally, the band at 2196 cm^{-1}, assigned to 2228 cm^{-1} in the calculated spectrum, shows minimal contribution from the C_9N_{13} motion. In this case, the PED encompassing C_9N_{13} appears to be very small and is not reported by VEDA. These observations suggest significant contributions from more distant nitrile groups due to the surface effect of AgNP. Considering the Ag-N_{13} model, the furthest nitrogen atom is ca. 1 nm from the AgNP. These discrepancies in relative intensities are expected due to model limitations in ignoring the SERS surface selection rule, which could allow considerations on the surface orientation, and they do not take into account the electromagnetic contribution. These factors could be responsible for the differences observed between the predicted and experimental relative intensities.

To investigate whether the presence of more Ag atoms on the complex model could allow for more complex coordination with the CDSQ, simulations were performed using a cluster of four Ag atoms (Ag_4). Two models for the geometry of coordination of CDSQ with the Ag_4 cluster are proposed: monodentate and bidentate coordination, where nitrogen acts as a ligand between CDSQ and Ag_4. The optimized geometries of the model complexes together with the simulated spectra and experimental SERS spectrum of CDSQ were presented in Figure 7. Tables S11-S14 include the atomic coordinates of the optimized structure and the structural parameters

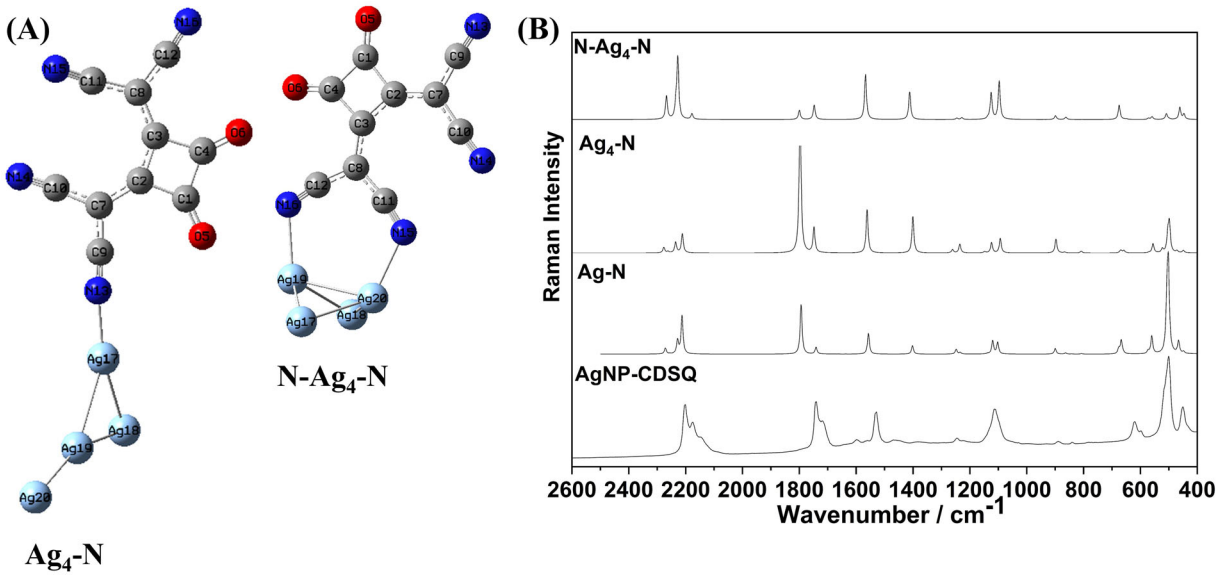

FIGURE 7 Optimized structures of different models for adsorption with cluster Ag_4 **(a),** and theoretical spectra and experimental SERS spectrum of CDSQ (b).

of each model. The incorporation of more silver atoms in the monodentate model did not result in significant changes in the vibrational signature of the CDSQ compound; only changes in the relative intensities of the Raman bands were observed. Furthermore, the analysis of the spectral profile for the bidentate coordination model also showed agreement with the number of bands present in the experimental data, emphasizing that this coordination may also be possible. However, in terms of relative Raman intensities, the bidentate coordination model shows more divergence from the experimental results. As observed, unlike the monodentate Ag-N model, the calculated Raman spectra considering the bidentate coordination of CDSQ with Ag atoms do not exhibit good agreement with the SERS results compared to the normal Raman spectrum. For instance, they fail to predict an intense carbonyl stretching band in the 1700–1800 cm^{-1} spectral region. The presence of the intense band located at 1794 cm^{-1}, attributed to the vibration ν (CC) + ν (CO), in the simulated spectrum for the monodentate model, suggests that the monodentate coordination was the most predominant configuration. By comparing the three coordination models presented in Figure 7, it is evident that the simplest model, involving only one silver atom, captured the most relevant spectral characteristics observed experimentally.

It can be seen from the SERS spectrum in Figure 6a, that there is an increase in the relative intensity of the band assigned purely to the CN stretching mode. The bands at 2196 and 2222 cm^{-1} are strong in the SERS spectrum (Figure 5a), while they are weak in the normal Raman spectrum (Figure 5b). These bands are also shifted by +14 and +11 cm^{-1} relative to the normal Raman spectrum in solution. The CN stretching band at 2163 cm^{-1}, absent in the normal Raman spectrum, is also enhanced in the SERS spectrum. These spectral differences give support to the adsorption of the CDSQ molecule through the interaction of a cyano group with the silver surface. It has been generally accepted in the literature that when CN groups interact with the electrons from lone pairs of nitrogen atoms (linear coordination; sigma donation).[46,47] Experimentally, there is an increase in the wavenumber of the CN stretching bands relative to the free molecule. This phenomenon can be attributed to the slight antibonding character of the nitrogen lone pair electrons, which play a significant role in the metal-adsorbate interaction and, consequently, strengthen the CN bonds during surface adsorption.[46] Therefore, the blue shift observed in its SERS spectrum for the ν (CN) modes indicates that the Na_2CDSQ molecule is adsorbed on the surface of Ag via the lone pairs of electrons of nitrogen. This result agrees with previous observations in the SERS studies of benzonitrile[48] and α-cyano-4-hydroxycinnamic acid.[46]

The DFT simulated spectra compared to the experimental results showed that there is no evidence of chemisorption of the CO group into Ag (Figure 6d). However, a significant band intensity increase is observed at 1761, 1550, and 260 cm^{-1}, which are attributed to the CO and CC vibration modes, suggesting that the aforementioned vibrational mode would present a large component perpendicular to the Ag surface.[27] It is quite reasonable, considering the CDSQ structure, that, if the CN group is perpendicular to the metal surface, the vibrational mode

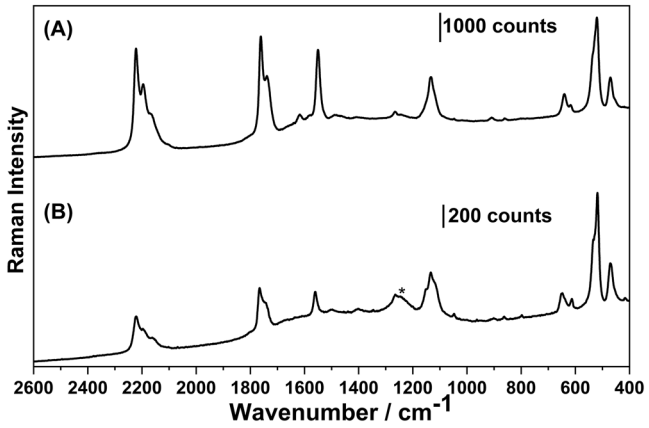

FIGURE 8 SERS spectra of the Na_2CDSQ solution were obtained at a concentration of 1.0 mmol L^{-1} (a) and 0.1 mmol L^{-1} (b). * Laser artifact at 785 nm.

of CO would also present large perpendicular components to the silver surface. This adsorption configuration explains the huge enhancement of such bands in the SERS spectrum.

In the sense to explore the sensitivity of the SERS technique, the SERS of Na_2CDSQ on the AgNP was investigated in one order of magnitude lower concentration, 0.1 mmol L^{-1}, as presented in Figure 8, compared to the spectrum at 1.0 mmol L^{-1}. It is important to note that, under the same experimental conditions, the SERS signal was not detectable at concentrations lower than 0.1 mmol L^{-1}. Therefore, the identification limit of the SERS signal for CDSQ was defined at 0.1 mmol L^{-1}.

It is noted that the overall SERS intensity decreases with the lowering of the Na_2CDSQ concentration. At 0.1 mmol L^{-1}, it is observed well-defined characteristic Na_2CDSQ bands, indicating that even at this concentration, the presence of the squaraine could still be detected with a reasonable signal-to-noise ratio. It can also be seen in Figure 8 that the intensity enhancement and wavenumber of the bands corresponding to the carbonyl and CN groups remained similar. These results provide strong evidence that the adsorption sites and structural conformation on the AgNP were not affected by a concentration of 0.1 mmol L^{-1}.

4 | CONCLUSIONS

In this work, we report for the first time the SERS spectra of the CDSQ solution. It used DFT calculations to support the vibrational assignments and for interpreting the SERS spectrum of the Na_2CDSQ obtained using AgNP suspensions. We have investigated by SERS the possibility of surface adsorption of CN and CO groups. The results have demonstrated that Na_2CDSQ is chemically adsorbed on the silver surface through one of its N atoms and that the molecule is placed perpendicular to the AgNP surface. From examining the (CN) band within SERS analysis, we have demonstrated that the blue shifts in SERS spectra for the bands at 2196 and 2222 cm^{-1} may be attributed to surface adsorption of the cyano, facilitated by the coordination of nitrogen lone-pair electrons. It was also suggested that the CO groups of CDSQ may be positioned close to the metal surface perpendicular to the surface conformation. Furthermore, we have verified the feasibility of obtaining the SERS signal of CDSQ at one order of magnitude lower concentration and verified a reasonable signal-to-noise ratio. This research contributes valuable information about the surface chemistry of CDSQ and may encourage further investigations into the properties and potential applications of this molecule for example in the field of organic solar cells.

AUTHORS' CONTRIBUTIONS

Flávia C. Marques: Methodology, Conceptualization, Validation, Investigation, Writing—original draft. Erix A. Milán-Garcés: Methodology, Formal analysis, Resources, Writing—review & editing. **Vanessa E. de Oliveira:** Methodology, Formal analysis, Resources, Writing—review & editing. **Stéfanos L. Georgopoulos:** Methodology, Writing—review & editing. **Gustavo F. S. Andrade:** Methodology, Formal analysis, Resources, Writing—review & editing. **Luiz Fernando C. de Oliveira:** Supervision, Conceptualization, Resources, Funding acquisition, Writing—review & editing.

ACKNOWLEDGEMENTS

The authors thank CNPq, FAPEMIG, and CAPES for their financial support. We are also indebted to Dr. Helio Ferreira dos Santos of the Núcleo de Estudos em Química Computacional (NEQC, at UFJF) for providing support for the execution of DFT calculations.

CONFLICT OF INTEREST STATEMENT

The authors declare that they have no known competing financial interests or personal relationships that could have appeared to influence the work reported in this paper.

ORCID

Flávia C. Marques https://orcid.org/0000-0003-1146-6597

Erix A. Milán-Garcés https://orcid.org/0000-0003-1134-7184

Vanessa E. de Oliveira https://orcid.org/0000-0002-6294-4782

REFERENCES

[1] J. He, Y. J. Jo, X. Sun, W. Qiao, J. Ok, T. Kim, Z. Li, *Adv. Funct. Mater.* **2021**, *31*, 2170077.

[2] E. Lima, L. V. Reis, *Future Med. Chem.* **2022**, *14*, 1375.

[3] K. Ilina, W. M. MacCuaig, M. Laramie, J. N. Jeouty, L. R. McNally, M. Henary, *Bioconjugate Chem.* **2020**, *31*, 194.

[4] S. Bellani, A. Iacchetti, M. Porro, L. Beverina, M. R. Antognazza, D. Natali, *Org. Electron.* **2015**, *22*, 56.

[5] K. Liang, K.-Y. Law, D. G. Whitten, *J. Phys. Chem.* **1995**, *99*, 16704.

[6] A. Broggi, H. Kim, J. Jung, M. P. Bracciale, M. L. Santarelli, C. Kim, A. Marrocchi, *Macromol. Chem. Phys.* **2017**, *218*, 1600487.

[7] A. J. McKerrow, E. Buncel, P. M. Kazmaier, *Can. J. Chem.* **1995**, *73*, 1605.

[8] D. Yang, Y. Jiao, L. Yang, Y. Chen, S. Mizoi, Y. Huang, X. Pu, Z. Lu, H. Sasabe, J. Kido, *J. Mater. Chem. A Mater.* **2015**, *3*, 17704.

[9] P.-L. Fabre, F. Dumestre, B. Soula, A.-M. Galibert, *Electrochim. Acta* **2000**, *45*, 2697.

[10] A. Tatarets, I. Fedyunyaeva, E. Terpetschnig, L. Patsenker, *Dyes Pigm.* **2005**, *64*, 125.

[11] A. Tripathi, C. Prabhakar, *Indian J Chem* **2018**, *57*, 1121.

[12] V. E. de Oliveira, G. S. de Carvalho, M. I. Yoshida, C. L. Donnici, N. L. Speziali, R. Diniz, L. F. C. de Oliveira, *J. Mol. Struct.* **2009**, *936*, 239.

[13] V. E. de Oliveira, M. C. R. Freitas, R. Diniz, M. I. Yoshida, N. L. Speziali, H. G. M. Edwards, L. F. C. de Oliveira, *J. Mol. Struct.* **2008**, *881*, 57.

[14] V. End de Oliveira, A. R. da Cunha, M. de Almeida Rizzutto, M. T. Lamy, L. F. C. de Oliveira, E. A. Milán-Garcés, *J. Phys. Chem. C* **2023**, *127*, 421.

[15] M. Ávila-Costa, C. L. Donnici, J. D. dos Santos, R. Diniz, A. Barros-Barbosa, A. Cuin, L. F. C. de Oliveira, *Spectrochim Acta a Mol Biomol. Spectrosc.* **2019**, *223*, 117354.

[16] S. L. Georgopoulos, E. A. Milán-Garcés, A. C. Sant'Ana, G. F. Souza Andrade, L. F. C. de Oliveira, *Vib. Spectrosc.* **2016**, *87*, 99.

[17] V. E. de Oliveira, R. Diniz, F. C. Machado, L. F. C. de Oliveira, in *Cross conjugation*, (Eds: H. Hopf, M. S. Sherburn) Vol. 32,Wiley, Weinheim, Germany **2016** 117.

[18] F. D. dos Reis, I. C. Gatti, H. C. Garcia, V. E. de Oliveira, L. F. C. de Oliveira, *J Phys Chem a* **2014**, *118*, 11521.

[19] C. E. Silva, H. F. Dos Santos, N. L. Speziali, R. Diniz, L. F. C. De Oliveira, *J. Phys. Chem. A* **2010**, *114*, 10097.

[20] C. E. Silva, R. Diniz, B. L. Rodrigues, L. F. C. de Oliveira, *J. Mol. Struct.* **2007**, *831*, 187.

[21] J. G. S. Lopes, R. A. Farani, L. F. C. De Oliveira, P. S. Santos, *Journal of Raman spectroscopy*, **2006**, *37*, 142.

[22] M. C. C. Ribeiro, L. F. C. de Oliveira, P. S. Santos, *Chem. Phys.* **1997**, *217*, 71.

[23] L. F. C. de Oliveira, P. S. Santos, *J. Mol. Struct.* **1992**, *269*, 85.

[24] L. F. C. Oliveira, P. S. Santos, *J. Mol. Struct.* **1991**, *263*, 59.

[25] P. S. Santos, J. H. Amaral, L. F. C. De Oliveira, *J. Mol. Struct.* **1991**, *243*, 223.

[26] R. Petry, M. Schmitt, J. Popp, *ChemPhysChem* **2003**, *4*, 14.

[27] E. L. R. P. Etchegoin, *Principles of surface-enhanced Raman spectroscopy and related plasmonic effects*, 1st ed., Elsevier Science, Amsterdam, Netherlands **2009**.

[28] M. Fan, G. F. S. Andrade, A. G. Brolo, *Anal. Chim. Acta* **2020**, *1097*, 1.

[29] M. Fan, G. F. S. Andrade, A. G. Brolo, *Anal. Chim. Acta* **2011**, *693*, 7.

[30] M. V. Cañamares, J. V. Garcia-Ramos, S. Sanchez-Cortes, M. Castillejo, M. Oujja, *J. Colloid Interface Sci.* **2008**, *326*, 103.

[31] R. Gupta, W. A. Weimer, *Chem. Phys. Lett.* **2003**, *374*, 302.

[32] K. Hering, D. Cialla, K. Ackermann, T. Dörfer, R. Möller, H. Schneidewind, R. Mattheis, W. Fritzsche, P. Rösch, J. Popp, *Anal. Bioanal. Chem.* **2008**, *390*, 113.

[33] F. C. Marques, G. P. Oliveira, R. A. R. Teixeira, R. M. S. Justo, T. B. V. Neves, G. F. S. Andrade, *Vib. Spectrosc.* **2018**, *98*, 139.

[34] B. Akbali, M. Yagmurcukardes, F. M. Peeters, H. Y. Lin, T. Y. Lin, W. H. Chen, S. Maher, T. Y. Chen, C. H. Huang, *J. Phys. Chem. C* **2021**, *125*, 16289.

[35] F. C. Marques, R. S. Alves, D. P. dos Santos, G. F. S. Andrade, *Phys. Chem. Chem. Phys.* **2022**, *24*, 27449.

[36] D. P. dos Santos, *J. Phys. Chem. C* **2020**, *124*, 6811.

[37] R. J. Stokes, A. Ingram, J. Gallagher, D. R. Armstrong, W. E. Smith, D. Graham, *Chem. Commun.* **2002**, *8*, 567.

[38] A. P. P. Alves, L. Á. De Sena, B. S. Archanjo, L. F. C. De Oliveira, S. D. O. Dantas, A. C. Sant'Ana, *Vib. Spectrosc.* **2013**, *64*, 153.

[39] N. Leopold, B. Lendl, *J. Phys. Chem. B* **2003**, *107*, 5723.

[40] M. J. Frisch, G. W. Trucks, H. B. Schlegel, G. E. Scuseria, M. A. Robb, J. R. Cheeseman, G. Scalmani, V. Barone, B. Mennucci, G. A. Petersson, H. Nakatsuji, M. Caricato, H. P. H. X. Li, A. F. Izmaylov, J. Bloino, J. L. S. G. Zheng, M. Hada, M. Ehara, K. Toyota, R. Fukuda, J. Hasegawa, M. Ishida, T. Nakajima, Y. Honda, O. Kitao, H. Nakai, T. Vreven, J. A. Montgomery, J. E. P. Jr, F. Ogliaro, M. Bearpark, J. J. Heyd, E. Brothers, K. N. Kudin, V. N. Staroverov, R. Kobayashi, K. R. J. Normand, A. Rendell, J. C. Burant, S. S. Iyengar, J. Tomasi, M. Cossi, N. Rega, J. M. Millam, M. Klene, J. E. Knox, J. B. Cross, V. Bakken, C. Adamo, J. Jaramillo, R. Gomperts, R. E. Stratmann, O. Yazyev, A. J. Austin, R. Cammi, C. Pomelli, J. W. Ochterski, R. L. Martin, K. Morokuma, V. G. Zakrzewski, G. A. Voth, P. Salvador, J. J. Dannenberg, S. Dapprich, A. D. Daniels, Ö. Farkas, J. B. Foresman, J. V. Ortiz, J. Cioslowski, and D. J. Fox, Wallingford.

[41] L. E. Roy, P. J. Hay, R. L. Martin, *J. Chem. Theory Comput.* **2008**, *4*, 1029.

[42] C.-H. Ho, S. Lee, *Colloids Surf. A Physicochem. Eng. Asp.* **2015**, *474*, 29.

[43] M. H. Jamróz, *Spectrochim. Acta. A Mol. Biomol. Spectrosc.* **2013**, *114*, 220.

[44] Y. Tawada, T. Tsuneda, S. Yanagisawa, T. Yanai, K. Hirao, *J. Chem. Phys.* **2004**, *120*, 8425.

[45] A. D. Becke, *J. Chem. Phys.* **1993**, *98*, 5648.

[46] D. Jung, K. Jeon, J. Yeo, S. Hussain, Y. Pang, *Appl. Surf. Sci.* **2017**, *425*, 63.

[47] H. Aee Chun, M. Soo Kim, K. Kim, *J. Mol. Struct.* **1990**, *221*, 127.

[48] D. W. Boo, K. Kim, M. S. Kim, *Bull. Korean Chem. Soc.* **1987**, *8*, 251.

SUPPORTING INFORMATION

Additional supporting information can be found online in the Supporting Information section at the end of this article.

How to cite this article: F. C. Marques, E. A. Milán-Garcés, V. E. de Oliveira, S. L. Georgopoulos, G. F. S. Andrade, L. F. C. de Oliveira, *J Raman Spectrosc* **2024**, 1. https://doi.org/10.1002/jrs.6716